

Numerical Simulations on Film Cooling Effectiveness from Two Staggered Rows of Coolant Jets



Z. Shu, C. Dai and J. Mi

Abstract This paper reports numerical simulations of the film cooling performance and flow structure from two staggered rows of coolant jets. The RANS modeling is conducted for the cases that are validated by and matched to the measurements of Sinha et al. (J Turbomach 113:442, 1991) [8]. The cooling effectiveness of two rows of jets is calculated for blowing ratios of 0.5 and 1.0. It is found that the interaction of counter-rotating vortex pairs (CRVPs) generated by two rows of jets enhances the cooling effectiveness significantly. Moreover, the calculations quantify the contribution from each row of coolant jets to the overall cooling performance and find that the second row makes more contribution than does the first row.

Keywords Jet in crossflow · Film cooling · RANS

1 Introduction

The modern gas turbine engines operate at extremely high temperature to improve efficiency. Often, the achievable temperature exceeds the metallurgical limit of the turbine blades' material, urgently requiring for effective blade cooling technique. As one of the most common and widely used techniques, film cooling has been investigated both experimentally [8, 9] and numerically [3, 4, 7] over half a century. The simple configurations cannot meet the demand as the cooling effectiveness decreases gradually downstream due to jet lift-off and mixing with hot freestream. Therefore, several studies were conducted with complex configurations of holes, such as sister holes proposed by Ely and Jubran [2] and two rows of holes investigated by Jung and Hennecke [6].

Z. Shu · C. Dai · J. Mi (✉)

Department of Energy & Resource Engineering, College of Engineering,
Peking University, Beijing, China
e-mail: jmi@pku.edu.cn

The previous studies have not yet investigated the process of interaction and also not quantified the contribution of each row of holes. The present work is to fill the deficit. A novel numerical method developed by Dai et al. [1] is applied to quantify contribution from each row to the overall cooling performance with a two staggered rows of coolant jets. In that method, the working fluids from various sources are marked by different artificial fluids with identical physical properties.

2 Computational Details

The work of Sinha et al. [8] is taken as the benchmark for the present work. The schematic of film cooling geometry and the boundary condition are provided in Fig. 1a, b. The streamwise, spanwise and vertical coordinates are denoted by X, Y and Z, respectively, with their origin at the jet exit center of side hole in the first row. The computational domain extends from freestream to two staggered rows of holes and two coolant plenums. The holes, each with diameter of $D = 12.7$ mm and length of $1.75D$, are inclined at 35° to the XY-plane. The ratios $P/D = 3.0$ and $S/D = 10.0$, where $P =$ pitch and $S =$ spacing. The velocity and temperature of freestream are 20 m/s and 300 K. The coolant temperature is 250 K to satisfy the constant density ratio of $DR = 1.2$. By varying the coolant velocity, we simulate the cases at blowing ratios of $M = 0.5$ and 1.0, where $M = DR(V_c/V)$. The Reynolds-Averaged Navier-Stokes (RANS) equations are solved with Ansys Fluent. The realizable $k-\epsilon$ model combined with the SIMPLEC algorithm are used to predict the film cooling effectiveness, while the QUICK solution scheme is applied to improve the calculation accuracy. Furthermore, to quantify contributions of the coolant jets from the first and second rows to the cooling effectiveness, a novel newly-developed simulation method is applied. The working fluid from the freestream and the first-row and second-row jets are marked, respectively, by real material air, artificial material air-row1 and air-row2. The artificial materials have the same physical properties as the real air. The cooling performance is mainly focused on the adiabatic effectiveness defined by

$$\eta = (T_\infty - T_{aw}) / (T_\infty - T_c) \quad (1)$$

where T , T_c , and T_{aw} are the temperatures of the freestream, coolant jets and adiabatic wall. The laterally averaged film cooling effectiveness $\bar{\eta}$ is calculated by integrating the cooling effectiveness along Y-direction of the wall, defined by

$$\bar{\eta} = \frac{1}{6D} \int_0^{6D} \eta(X, Y) dY. \quad (2)$$

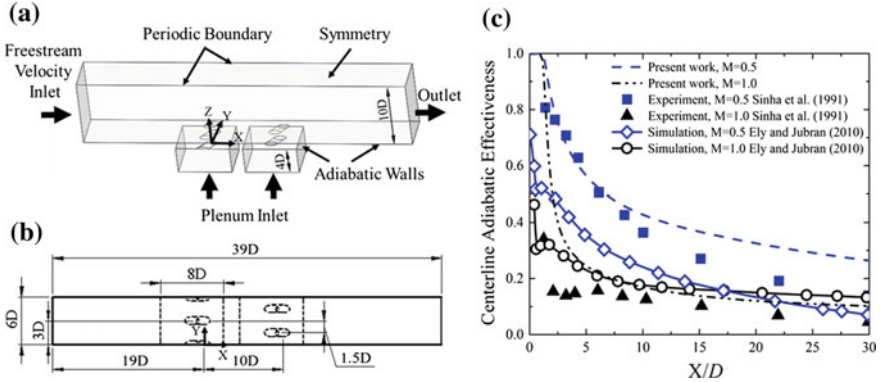


Fig. 1 Physical domain and boundary conditions: a 3-D, b top view; c Streamwise variation of the centerline adiabatic effectiveness

3 Results and Discussion

3.1 Validations

To validate the model setting of computation, Fig. 1c compares our predictions of the centerline adiabatic effectiveness η of a single row of holes for $M = 0.5$ and 1.0 with the measurements of Sinha et al. [8]. Displayed are also the predictions of Ely and Jubran [3]. Our numerical results agree reasonably well with the experimental data for the two cases, despite the overprediction occurring for $M = 1.0$ at all X and for $M = 0.5$ at $X > 8D$. The similar overprediction was found by Johnson et al. [5] and Khajehhasani and Jubran [7]. The reason is that the $k-\epsilon$ model of turbulence improperly uses the isotropic assumption of eddy diffusivity, see Johnson et al. [5]. Below, the interaction of jets from two staggered rows is investigated with the same settings.

3.2 Adiabatic Cooling Effectiveness

Figure 2a compares the streamwise variations of the lateral average of η for two rows of jets at $M = 0.5$ and 1.0 . Evidently, the cooling effectiveness is higher for $M = 0.5$ than for $M = 1.0$ all the way at $X/D < 25$. It is also demonstrated that the cooling becomes more effective downstream from the second row ($X > 10D$) in both cases. Figure 2b shows distributions of local η to quantify the cooling performance in the whole adiabatic wall. For $M = 0.5$, the jets are closely attached to the wall and penetrate to the freestream. The cooling effectiveness drops gradually downstream as coolant mixes with hot freestream. For $M = 1.0$, as the flow proceeds downstream, the cooling effectiveness starts with a very low value near the

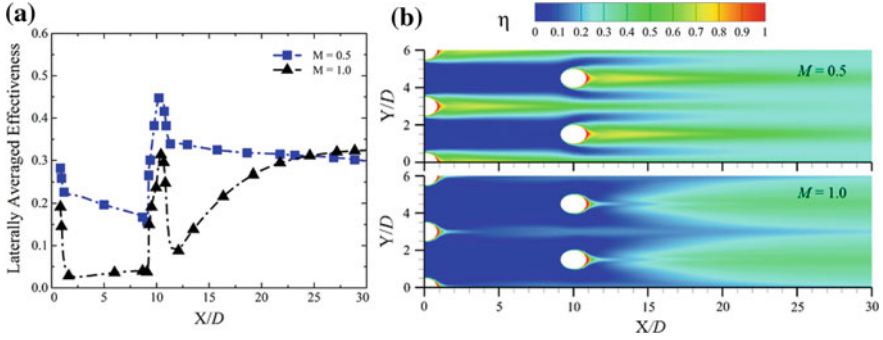


Fig. 2 Effectiveness of two row jets for $M = 0.5$ and 1.0 : **a** streamwise variation of laterally averaged effectiveness; **b** contours of local adiabatic film cooling effectiveness

hole exit and then increases monotonically. The reason follows. As jets penetrate into the freestream, their lift-off occurs initially, due to high momentum. Consequently, almost no coolant touches and cools the surface. Farther downstream, the original lift-off coolant jets are reattached to the wall, thus increasing the cooling effectiveness. The effectiveness of $M = 1.0$ is even higher than that for $M = 0.5$ at $X > 25D$ because of larger coolant mass.

3.3 Interaction of Two-Row Jets

Figure 3 displays distributions of the streamwise vorticity together with streamlines at various locations for $M = 1.0$. The figure shows evolutions of counter-rotating vortex pairs (CRVPs) generated from the two rows of holes. As seen in Fig. 3c, d, the nearby CRVP of the first row is spinning in opposite direction, which pushes the CRVP of the second row closer to the wall. Besides, the gap of the second row of holes is filled by the coolant from the first row, then the CRVP of the second row entrains the relatively low temperature coolant instead of the hot freestream. Therefore, the entrainment of the CRVP make the coolant from both rows more uniform in lateral direction, see Fig. 4a and b. Here, X_{c1} and X_{c2} represent the coolant mass fractions from the first and second row, respectively. The lift-off and reattachment also can be observed. The reattachment occurs sufficiently downstream of both rows but is more pronounced downstream of the second row due to the interaction of jets. Figure 4c shows the total mass fraction of coolant $X_c (= X_{c1} + X_{c2})$ and local cooling effectiveness η . Since cooling effectiveness is closely related to the local mass fraction of coolant, η is almost identical with X_c . To quantify the contribution of each row, Fig. 4d displays the lateral distributions of $\eta_1 = X_{c1}/X_c\eta$ and $\eta_2 = X_{c2}/X_c\eta$, i.e., the cooling effectivenesses from the first and

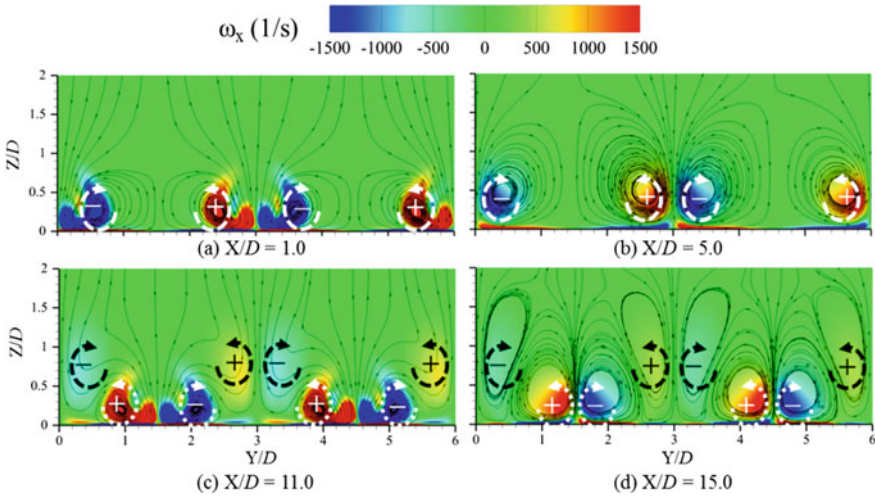


Fig. 3 Streamwise vorticity and streamline distribution for $M = 1.0$ at **a** $X/D = 1.0$, **b** $X/D = 5.0$, **c** $X/D = 11.0$ and **d** $X/D = 15.0$

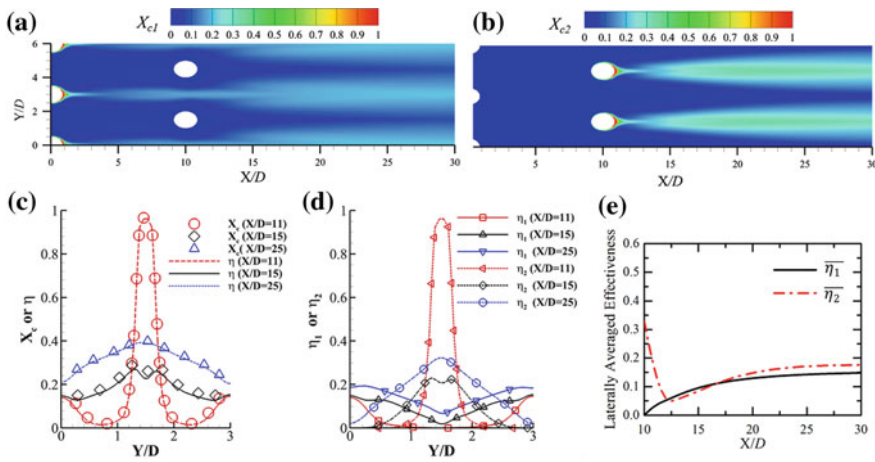


Fig. 4 Local mass fraction distributions of coolant from **a** the first row X_{c1} and **b** the second row X_{c2} . **c** Total mass fraction of coolant X_c and η at $X/D = 11, 15$ and 25 . **d** Cooling effectiveness generated by coolant of the first row η_1 and that of the second row η_2 at $X/D = 11, 15$ and 25 . **e** Laterally averaged cooling effectiveness of the first row $\overline{\eta_1}$ and the second row $\overline{\eta_2}$

second row, while Fig. 4e reports on the average cooling effectiveness $\overline{\eta_1}$ and $\overline{\eta_2}$ at different locations. Clearly, η_2 is much higher than η_1 downstream of the second row at $1D < Y < 2D$ but is lower at the sides of the hole exit. Generally, see Fig. 4e, the average contribution of the second row is greater than that of the first row.

4 Conclusion

This numerical work has investigated the film cooling performance and flow structure from two staggered rows of jets. The significant interaction of two rows results mainly from the entrainment between the CRVPs of two rows, making the coolant mass distribution more uniform laterally than the single row injection. By quantifying the contribution from each row to the overall cooling performance, the second row is found to make more contribution than does the first row.

Acknowledgements The support of National Key Research and Development Program of China (No.: 2016YFB0600605) is gratefully acknowledged.

References

1. Dai C, Shu Z, Mi J (2017) Quantitative investigation on the formation of counter-rotating vortex pairs from the inclined jet in crossflow. In: The 4th symposium on FSSIC-No. 112 (accepted)
2. Ely MJ, Jubran BA (2008) A numerical study on increasing film cooling effectiveness through the use of sister holes. In: ASME conference proceedings 2008, pp 341–350
3. Ely MJ, Jubran BA (2010) A parametric study on the effect of sister hole location on active film cooling flow control. ASME
4. Goldstein RJ, Eckert ERG, Burggraf F (1974) Effects of hole geometry and density on three-dimensional film cooling. *Int J Heat Mass Transf* 17:595–607
5. Johnson PL, Shyam V, Hah C (2011) Reynolds-averaged Navier-Stokes solutions to flat plate film cooling scenarios. Nasa/Tm
6. Jung K, Hennecke DK (2001) Curvature effects on film cooling with injection through two rows of holes. *Tro-Mp-069(I)* 069, 6 1–14
7. Khajehhasani S, Jubran BA (2014) Numerical assessment of the film cooling through novel sister-shaped single-hole schemes. *Numer Heat Transf Part A: Appl* 67:414–435
8. Sinha AK, Bogard DG, Crawford ME (1991) Film-cooling effectiveness downstream of a single row of holes with variable density ratio. *J Turbomach* 113:442
9. Yazid MH, Hamidon BS, Razali A (2015) An experiment investigation of film cooling effectiveness of sister hole of cylindrical shaped hole film cooling geometry on a flat plate surface, pp 3–7